Loss of MIG-6 results in endometrial progesterone resistance via ERBB2

Jung-Yoon Yoo
Yonsei University
Tae Hoon Kim
Michigan State University
Jung-Ho Shin
Guro Hospital, Korea University Medical Centre
Ryan Marquardt
Michigan State University https://orcid.org/0000-0002-6597-4506
Ulrich Mueller
Johns Hopkins University
Asgerally Fazleabas
Michigan State University
Steven Young
University of North Carolina https://orcid.org/0000-0002-5205-4495
Bruce Lessey
Wake Forest Baptist Medical Center
Ho-Geun Yoon
Yonsei University College of Medicine, https://orcid.org/0000-0003-2718-3372
Jae-Wook Jeong (jeongj@msu.edu)
Michigan State University

Article

Keywords:

Posted Date: November 10th, 2020

DOI: https://doi.org/10.21203/rs.3.rs-95903/v1

Version of Record: A version of this preprint was published at Nature Communications on March 1st, 2022. See the published version at https://doi.org/10.1038/s41467-022-28608-x.

Abstract

Female subfertility is highly associated with endometriosis. Although the exact etiology of endometriosis-related infertility remains to be determined, endometrial progesterone resistance has recently been suggested as a crucial element in the development of endometrial diseases. Here, we report that *MIG-6*, a progesterone-induced gene, is downregulated in the endometrium of infertile women with endometriosis and in a non-human primate model of endometriosis. In an endometriosis mouse model with a fluorescent reporter used to identify lesions, an increase of endometriosis development and implantation failure were observed in mice with *Mig-6* deficient endometrium compared to controls. MIG-6 is known to inhibit ERBB2, which we found overexpressed in the endometrium from uterine-specific *Mig-6* knock-out mice ($Pgr^{cre/+}Mig\text{-}6^{f/f}$; $Mig\text{-}6^{d/d}$). To investigate the effect of ERBB2 targeting on endometrial progesterone resistance, fertility, and endometriosis, we introduced *Erbb2* ablation in $Mig\text{-}6^{d/d}$ mice ($Mig\text{-}6^{d/d}Erbb2^{d/d}$ mice). The additional knockout of *Erbb2* rescued all phenotypes seen in $Mig\text{-}6^{d/d}$ mice including endometrial progesterone resistance, infertility, and endometriosis lesion development. Transcriptomic analysis showed that genes differentially expressed in $Mig\text{-}6^{d/d}$ mice reverted to their normal expression amounts in $Mig\text{-}6^{d/d}Erbb2^{d/d}$ mice. Together, our results demonstrate that MIG-6-induced ERBB2 overexpression causes endometrial progesterone resistance and a nonreceptive endometrium in endometriosis-related infertility and that ERBB2 targeting reverses these effects.

Introduction

Critical for fertility, the uterine endometrium's epithelial and stromal compartments undergo dynamic hormonally controlled molecular and morphological changes to prepare for embryo implantation and development. Estrogen (E2) stimulates the proliferation of uterine epithelial cells, and progesterone (P4) suppresses E2-induced proliferation. Endometrial P4 resistance implies decreased responsiveness of target tissue to bioavailable P4 [1, 2, 3]. Endometrial P4 resistance is seen in women with a nonreceptive endometrium, endometriosis, polycystic ovary syndrome (PCOS), and endometrial cancer [4, 5, 6, 7, 8, 9]. Moreover, P4-induced molecular changes in the eutopic (intrauterine) endometrial tissue of women with endometriosis are either blunted or undetectable [10, 11, 12].

Endometriosis affects about 10% of all women of reproductive age, and the incidence increases to 50–60% of women with chronic pelvic pain and infertility [13, 14]. While progestin-based therapies are commonly used to treat endometriosis and lead to disease regression in some women, other women with endometriosis and pelvic pain do not respond effectively to progestins [15, 16]. Moreover, many P4-induced molecular changes in the eutopic endometrial tissue of women with endometriosis are either blunted or dysregulated [17, 18], but an impaired P4 response is seen in the endometrium of women with endometriosis [4, 5, 6, 10]. Despite knowing the effects, the molecular mechanism responsible for endometrial P4 resistance and dysregulation remains unclear. Therefore, understanding the molecular mechanisms of endometrial P4 resistance is critical.

The present study revealed that the amount of mitogen inducible gene 6 (MIG-6) was decreased in endometrium from infertile women with endometriosis. We used uterine-specific *Mig-6* knock-out mice to demonstrate that MIG-6 loss results in endometrial progesterone resistance via ERBB2. Our findings provide new insight into the etiology of female infertility and provide a new molecular framework useful for the design of new therapeutic strategies.

Results

MIG-6 expression is decreased in endometrium from women with endometriosis.

We previously identified *Mig-6* as a P4-regulated gene that mediates the ability of P4 to repress E2 action in the mouse uterus [19, 20]. During the menstrual cycle, P4 amounts rise at the early secretory phase. As measured by RT-qPCR, *MIG-6* expression in the human endometrium was significantly higher in the early secretory phase of the menstrual cycle than in the proliferative phase ($p < 0.001$) (Fig. 1A), suggesting that *MIG-6* is a P4-induced gene in the human endometrium as has been demonstrated in the mouse [20]. Because many P4-induced endometrial molecular changes are either blunted or eliminated in women with endometriosis [1, 5, 8], we examined MIG-6 expression in endometrial biopsies from infertile women with endometriosis. RT-qPCR and immunohistochemistry showed that amounts of *MIG-6* mRNA ($p < 0.01$) and protein ($p < 0.001$) were significantly lower in the eutopic endometrium of infertile women with endometriosis compared to controls in the early secretory phase (Fig. 1, A-C). To assess how MIG-6 expression is affected by endometriosis progression, we used a baboon model [21]. Intraperitoneal inoculation with autologous menstrual effluent in female non-human primates results in formation of endometriotic lesions highly similar in histomorphology to those seen in women [22]. We found that endometrial MIG-6 protein abundance was significantly reduced in baboons during the progression of endometriosis after experimental disease induction as compared to paired pre-inoculation control samples (Fig. 1D; $p < 0.001$). These results demonstrate that reduced MIG-6 expression can be caused by the development of endometriotic lesions.

Uncovering pathophysiological mechanisms of endometriosis-related infertility with animal models requires easy identification of lesions to distinguish them from the surrounding normal tissues. With this in mind, we developed a mouse model of endometriosis using *mT/mG* reporters. In $Pgr^{cre/+}Rosa26^{mTmG/+}$ mice, progesterone receptor (*Pgr*)-positive uterine cells express mG, while *Pgr*-negative cells express mT (fig. S1 A and B). Using this model, we surgically induced endometriosis in $Pgr^{cre/+}Rosa26^{mTmG/+}$ mice by inoculating autologous endometrial tissue fragments into the peritoneal cavity after 3 days of E2 treatment (fig. S1C). This method leads to the development of endometriotic lesions similar to those in humans without the need for ovariectomy or unopposed E2 treatment (fig. S1 D-F). To examine the responsiveness of our endometriosis model to E2 and P4, $Pgr^{cre/+}Rosa26^{mTmG/+}$ mice induced with endometriosis were treated with vehicle, E2, or E2 + P4 for 2 weeks. While E2 treatment after endometriosis induction significantly increased the number of endometriotic lesions compared to the vehicle group, the addition of P4 suppressed the E2-induced increase in lesion number (fig. S1 G and H; p

< 0.01). Our mouse model thus closely mirrors human endometriosis as an E2-dependent and P4-suppressed disorder. To determine whether MIG-6 expression is dysregulated after endometriosis development in a distinct mammalian system, we examined MIG-6 amount in the eutopic endometrium from *Pgr*$^{cre/+}$*Rosa26*$^{mTmG/+}$ mice with endometriosis. MIG-6 protein expression was significantly reduced in eutopic endometrium from the mice with endometriosis compared to the sham group (Fig. 1E; $p < 0.001$).

Mig-6 loss accelerated the development of endometriosis and endometriosis-related infertility.

Next, we assessed whether endometriosis in mice causes infertility by assessing implantation and decidualization success. One month after endometriosis induction, the number of implantation sites in mice with endometriosis was not changed compared to the sham group. However, 63.6% (7 out of 11) of mice with endometriosis experienced implantation failure 3 months after endometriosis development (fig. S2A). We next examined the impact of endometriosis on decidualization using an artificial decidualization model [23]. One month after endometriosis induction, mice with endometriosis displayed a uterine horn that responded well to artificial decidualization; however, after 3 month of endometriosis development, the mice with endometriosis exhibited a significant defect in decidual response compared to control and sham mice (fig. S2B; $p < 0.001$). Our result suggests that endometriosis development causes implantation failure and a defect of decidualization, as has been hypothesized in humans [5].

Having established the link between endometriosis development and MIG-6 attenuation in the eutopic endometrium, we sought to determine if MIG-6 depletion is involved in endometriotic lesion development. In a comparison of MIG-6 expression in paired ectopic and eutopic endometrial biopsies taken from women with endometriosis, MIG-6 amounts were significantly reduced in the ectopic endometrial specimens ($p < 0.01$) (Fig. 2A and B). To assess the effect of MIG-6 deficiency in endometriosis development, we induced endometriosis in control (*Pgr*$^{cre/+}$*Rosa26*$^{mTmG/+}$) and *Mig-6*$^{d/d}$*Rosa26*$^{mTmG/+}$ mice and found that uterine MIG-6 attenuation significantly increased incidence ($p < 0.01$) and weight of endometriotic lesions ($p < 0.05$) (Fig. 2C and D). To address the role of MIG-6 in endometriosis-related infertility, we surgically induced endometriosis in wild type females using endometrial fragments from donor control (*Pgr*$^{cre/+}$*Rosa26*$^{mTmG/+}$) and *Mig-6*$^{d/d}$*Rosa26*$^{mTmG/+}$ mice (Fig. 2E). One month after endometriosis induction, the number of implantation sites was significantly reduced in the mice with *Mig-6*$^{d/d}$*Rosa26*$^{mTmG/+}$ ectopic lesions compared to the mice with control ectopic lesions ($p < 0.05$). Furthermore, implantation sites were entirely absent from mice with *Mig-6*$^{d/d}$*Rosa26*$^{mTmG/+}$ ectopic lesions after 2 months of endometriosis development (Fig. 2F and G). These results demonstrate that MIG-6 attenuation in ectopic lesions increased endometriosis development and accelerated implantation failure compared to controls.

Cessation of epithelial E2-induced proliferation is essential for implantation in all eutherian mammal species studied [24, 25]. In mice, abundant proliferation of epithelial and stromal cells is detectable at day 2.5 of gestation (GD 2.5). However, just before implantation, P4 inhibits epithelial proliferation and

induces differentiation to an embryo receptive state [26]. Establishing uterine receptivity by sequential actions of E2 and P4 on endometrial cells is critical for successful embryo apposition, attachment, implantation, and pregnancy maintenance, and lack of sufficient E2 and P4 action can result in infertility and pregnancy loss in humans [5, 7, 10, 27] and mice [28, 29, 30, 31]. *Mig-6*$^{d/d}$ mice are infertile due to P4 resistance and implantation failure [32]. To determine whether a defect of embryo implantation is caused by an alteration in endometrial cell proliferation, we examined expression of a proliferation marker (Ki67) at pre-implantation (GD 3.5). Epithelial proliferation was significantly increased in the *Mig-6*$^{d/d}$ endometrium compared to controls ($p < 0.001$) (*Mig-6*$^{f/f}$; fig. S3 A and B). To identify the molecular explanation for the effect of MIG-6 loss on epithelial proliferation, we examined amounts of several E2 signaling molecules, including epidermal growth factor receptor (EGFR), erb-b2 receptor tyrosine kinase 2 (ERBB2; also known as CD340, proto-oncogene Neu, or HER2) and extracellular-signal-regulated kinase 1/2 (ERK1/2) at GD 3.5 in *Mig-6*$^{f/f}$ and *Mig-6*$^{d/d}$ mice. EGFR amounts were unchanged, but ERBB2 and phospho-ERK1/2 (pERK1/2) amounts were selectively increased in *Mig-6*$^{d/d}$ mice (fig. S3 C and D). These results suggest MIG-6 is a negative regulator of ERBB2/ERK signaling in the pre-implantation endometrium.

Erbb2 overexpression causes infertility seen in Mig-6 mutant mice.

In order to investigate the effect of ERBB2 targeting on nonreceptive endometrium and endometriosis with *Mig-6* deficiency, we introduced *Erbb2* ablation in *Mig-6*$^{d/d}$ mice (*Mig-6*$^{d/d}$*Erbb2*$^{d/d}$; fig. S4). To address the effect of conditional *Erbb2* knockout on the infertility phenotype of *Mig-6*$^{d/d}$ mice, we mated female control, *Mig-6*$^{d/d}$, and *Mig-6*$^{d/d}$*Erbb2*$^{d/d}$ (*Pgr*$^{cre/+}$*Mig-6*$^{f/f}$*Erbb2*$^{f/f}$) mice with wild type male mice for 6 months to determine their overall fertility. As expected, *Mig-6*$^{d/d}$ mice were infertile [20], but surprisingly, *Mig-6*$^{d/d}$*Erbb2*$^{d/d}$ exhibited normal fecundity compared to controls (6.40 ± 0.49 and 7.29 ± 0.29 average pups/litter, respectively; table S1). This is the first report of molecular targeting to correct infertility caused by endometrial P4 resistance.

To further dissect the reversal of *Mig-6*-related infertility by attenuation of *Erbb2*, we examined implantation rates. Uterine horns of *Mig-6*$^{d/d}$ mice had no grossly visible implantation sites at GD 5.5, whereas *Mig-6*$^{d/d}$*Erbb2*$^{d/d}$ mice averaged 7.00 ± 0.41 implantation sites that appeared normally spaced (Fig. 3A). Subsequent histology revealed all embryos in *Mig-6*$^{d/d}$*Erbb2*$^{d/d}$ uteri were positioned as expected alongside the anti-mesometrial luminal epithelium, and the stromal cells had the normal decidual response surrounding the embryo (Fig. 3B). To identify the effect of additional *Erbb2* knockout on the aberrantly increased epithelial proliferation of GD 3.5 *Mig-6*$^{d/d}$ mice, we assessed Ki67 and cyclin D1 expression in *Mig-6*$^{d/d}$*Erbb2*$^{d/d}$ mice. In contrast to *Mig-6*$^{d/d}$ mice, *Mig-6*$^{d/d}$*Erbb2*$^{d/d}$ endometrial epithelial cells exhibited normal cyclin D1 and Ki67 (Fig. 3C). Since the increase of epithelial proliferation in *Mig-6*$^{d/d}$ mice is accompanied by increased E2 signaling, we investigated whether excess E2 signaling is abrogated by *Erbb2* ablation. The expression of the E2-responsive genes mucin 1 (*Muc-1*) ($p < 0.001$), chloride channel calcium activated 3 (*Clca3*)($p < 0.01$), lactoferrin (*Ltf*)($p < 0.001$), and complement

component 3 (*C3*) ($p < 0.05$) were significantly increased in *Mig-6*$^{d/d}$ mice but restored to normal amounts in *Mig-6*$^{d/d}$*Erbb2*$^{d/d}$ mice (Fig. 3D). The same pattern was apparent for MUC1 and LTF protein amounts (Fig. 3E). These results imply that ERBB2 overexpression resulting from *Mig-6* attenuation causes female infertility due to a nonreceptive endometrium, and this effect may be reversed by ablation of *Erbb2.*

Erbb2 ablation overcomes P4 resistance in Mig-6 mutant mice.

Mig-6 attenuation causes endometrial P4 resistance demonstrated by P4's inability to inhibit E2-induced uterine weight gain in *Mig-6*$^{d/d}$ mice [20]. In order to determine if *Erbb2* ablation restores endometrial P4 responsiveness in *Mig-6*$^{d/d}$ mice, ovariectomized control, *Mig-6*$^{d/d}$, and *Mig-6*$^{d/d}$*Erbb2*$^{d/d}$ mice were treated with vehicle or E2 + P4 for 3 days. While *Mig-6*$^{d/d}$ mice treated with E2 + P4 experienced significant increases in uterine weight ($p < 0.05$), vascularization, and expression of the E2 target genes *Muc1*, *Clca3*, *Ltf*, and *C3* compared to E2 + P4 treated control mice ($p < 0.001$), *Mig-6*$^{d/d}$*Erbb2*$^{d/d}$ mice exhibited normal P4 responsiveness and expression of E2 target genes (Fig. 4, A-C). We then examined the effect of *Erbb2* ablation in the endometriosis development of *Mig-6*$^{d/d}$ mice and found the number and weight of endometriotic lesions were restored to control amounts by the additional ablation of *Erbb2* (Fig. 4D and E; fig. S5).

Uterine *Mig-6* ablation causes endometrial hyperplasia by 5 months of age [20]. To investigate the impact of additional *Erbb2* knockout on endometrial hyperplasia development due to *Mig-6* attenuation, we examined uterine weight and gross histological morphology in control, *Mig-6*$^{d/d}$, and *Mig-6*$^{d/d}$*Erbb2*$^{d/d}$ mice at 5 months of age. Uterine weight was significantly decreased in *Mig-6*$^{d/d}$*Erbb2*$^{d/d}$ mice when compared to *Mig-6*$^{d/d}$ mice ($p < 0.001$), and histological analysis revealed that *Mig-6*$^{d/d}$*Erbb2*$^{d/d}$ mice did not develop endometrial hyperplasia (fig. S6). These results demonstrate that all known female reproductive phenotypes caused by knocking out uterine *Mig-6* are restored to baseline by also knocking out *Erbb2*.

To identify the signaling pathways that *Mig-6* regulates at pre-implantation, we performed transcriptomic analysis on the uteri from control, *Mig-6*$^{d/d}$, and *Mig-6*$^{d/d}$*Erbb2*$^{d/d}$ mice at GD 3.5. We found 1,022 and 771 increased or decreased transcripts, respectively, in the *Mig-6*$^{d/d}$ uterus as compared with controls (Fig. 5A and table S2). Remarkably, 1,722 of the altered genes (96.04%) in *Mig-6*$^{d/d}$ mice reverted to their normal expression amounts in *Mig-6*$^{d/d}$*Erbb2*$^{d/d}$ mice. Pathway analysis showed that major altered pathways in the *Mig-6*$^{d/d}$ uterus included cell-cycle control and DNA replication. P4 blocks E2-induced DNA synthesis by inhibiting replication licensing including mini-chromosome maintenance (MCM) proteins [33, 34] which have a role in both the initiation and elongation phases of eukaryotic DNA replication as part of the MCM complex [35, 36]. Fifteen genes associated with cell cycle and DNA replication were significantly changed in the *Mig-6*$^{d/d}$ uterus (table S3). RT-qPCR analysis confirmed that the additional knockout of *Erbb2* in *Mig-6*$^{d/d}$ mice restored dysregulated cell-cycle control and DNA-replication-related gene transcripts to normal (Fig. 5B). IHC results showed that at the protein level as well, aberrant

overexpression of MCM2 and MCM6 occurred in *Mig-6*$^{d/d}$ mice at the pre-implantation stage but reverted to normal in *Mig-6*$^{d/d}$*Erbb2*$^{d/d}$ mice (Fig. 5C). A similar action can be ascribed to P4 and E2 in the human endometrial epithelium, since a loss of MCM proteins occurs in the secretory phase, and P4 dominates this phase of the menstrual cycle [37]. Additionally, aberrant overexpression of MCM2 and MCM6 may cause abnormal epithelial proliferation and nonreceptive endometrium in infertile women with endometriosis [38]. Two Kruppel-like transcription factors (KLFs) are implicated in E2 and P4 modulation of uterine proliferation [38]. *Klf4* expression is increased by E2 and promotes DNA replication, whereas *Klf15* is increased by P4 and inhibits growth via regulation of *Mcm2* [38]. The expression of KLF4 was significantly increased in *Mig-6*$^{d/d}$ mice compared to control mice while the expression of KLF15 was decreased in *Mig-6*$^{d/d}$ mice, and the amounts reverted to normal in *Mig-6*$^{d/d}$*Erbb2*$^{d/d}$ mice ($p < 0.001$) (Fig. 5, B and D). These results suggest that *Erbb2* overexpression due to *Mig-6* ablation causes E2-induced epithelial proliferation and P4 resistance by disrupting cell cycle regulation.

Discussion

This study reveals the attenuation of MIG-6 in eutopic endometrium from infertile women with endometriosis compared to controls. MIG-6 expression was higher in human endometrium from the early secretory phase than in endometrium from the proliferative phase. Because of the complexity and dynamic nature of implantation, the molecular processes underlying these changes are poorly understood. Improving fertility rates requires unraveling molecular mechanisms of implantation. However, how regulation occurs between P4 and E2 is still not fully understood[39, 40], which is a critical barrier to better therapies for infertility. Amounts of MIG-6 mRNA and protein were lower in the eutopic endometrium of infertile women with endometriosis compared to controls in the early secretory phase. These results suggest that MIG-6 is a P4-responsive gene in human endometrium as in the mouse[20], and MIG-6 loss may result in a non-receptive endometrium in endometriosis-related infertility.

Nonhuman primates are advantageous for studying endometriosis because they are phylogenetically similar to humans[41, 42, 43]. Intraperitoneal inoculation with autologous menstrual effluent results in formation of endometriotic lesions similar in histology and morphology to those seen in women[22]. Paired sequential analysis showed MIG-6 protein amounts were decreased in the eutopic endometrium of baboons during progression of endometriosis as compared to pre-inoculation control. Furthermore, MIG-6 protein expression was reduced in the eutopic endometrium from the mice with endometriosis compared to the sham group. This result demonstrated reduced MIG-6 expression is associated with endometriosis development.

We developed a mouse model of endometriosis based on *Pgr*$^{cre/+}$ and *mT/mG* reporters that produces endometriotic lesions highly similar to those in humans. A mouse model in which excised human endometrial fragments are introduced into the peritoneum of immunocompromised mice is widely used, but is limited by lack of a normal immune system, which is thought to be important in endometriosis pathophysiology[44, 45, 46]. In contrast, the mouse model of induced endometriosis is a versatile model that

has been used to study how the immune system[47], hormones[48, 49] and environmental factors[50, 51] affect endometriosis. The availability of a large number of transgenic mice in which specific genes can be either eliminated or overexpressed make this induced endometriosis model ideal for studying specific pathways in development and progression of endometriosis and other diseases[46]. However, current mouse models of endometriosis that involve ovariectomy and E2 treatment are impractical for studies of physiological functions that require natural fluctuations in ovarian steroid hormones, such as fertility. On the other hand, our mouse model alleviates the need to apply ovariectomy and E2 treatment to enlarge endometriotic lesions because fluorescence reporter genes allow us to visualize *in vivo* and in real-time endometriotic lesions like those found in humans. Moreover, similarities between our mouse model and human endometriosis include: 1) development and progression of disease; 2) steroid hormone regulation; 3) fertility defect with implantation failure; and 4) P4 resistance in endometrium with *Mig-6* deficiency. Furthermore, the fluorescence reporters enable us to quantitatively examine endometriotic lesions in these mice more accurately and easily than in prior models.

Because *Mig-6*$^{d/d}$ mice have a fertility defect[20, 32], we applied a syngeneic mouse model to examine the effect of endometriotic lesions with *Mig-6* ablation on the eutopic endometrium. Several groups have used syngeneic mouse models of endometriosis, in which the uterus of one mouse is removed, minced and injected intraperitoneally into recipient mice[46]. Syngeneic murine models have several potential advantages over the rodent surgical model: 1) peritoneal seeding of uterine fragments is more similar to retrograde menstruation in women; 2) either the donor or recipient animal can receive therapeutic intervention or be otherwise manipulated prior to induction of disease; and 3) a large number of transgenic mice in which specific genes can be either eliminated or overexpressed are available. These advantages make syngeneic murine models ideal for studying the role of specific pathways in development and progression of endometriosis and other diseases.

P4 is absolutely required for uterine implantation, decidualization, and maintenance of pregnancy [8, 52]. How endometriosis contributes to infertility remains elusive, although P4 resistance is likely involved[1]. P4 resistance is seen in the endometrium of infertile women with endometriosis, and *Mig-6*$^{d/d}$ mice exhibit P4 resistance by the inability of P4 to inhibit E2-induced uterine weight gain[20]. We demonstrate that MIG-6 mediates P4 inhibition of E2-induced cell proliferation by inhibition of ErbB2-ERK signaling. MIG-6 plays an important role in inhibiting epithelial cell proliferation and facilitating implantation. Epithelial cell proliferation and cyclin D1 amounts were higher in the epithelial cells of *Mig-6*$^{d/d}$ mice, whereas both *Mig-6*$^{d/d}$*Erbb2*$^{d/d}$ and control mice lacked elevated cyclin D1 amounts and epithelial cell proliferation. These results suggest that MIG-6 is a negative regulator of ErbB2 and suppresses E2-induced epithelial cell proliferation at the pre-implantation stage.

We evaluated the potential therapeutic value of ErbB2 as a target for correcting endometrial P4 resistance in infertility. In our transcriptomic analysis in *Mig-6*$^{d/d}$ and *Mig-6*$^{d/d}$*Erbb2*$^{d/d}$ mice at GD 3.5, altered genes in *Mig-6*$^{d/d}$ mice reverted to their normal expression amounts in *Mig-6*$^{d/d}$*Erbb2*$^{d/d}$ mice. Pathway analysis using Ingenuity Systems Software showed that major altered pathways in the *Mig-6*$^{d/d}$ uterus included

cell-cycle control and DNA replication. Dr. Pollard's group showed that P4 blocks E2-induced DNA synthesis by inhibiting replication licensing including mini-chromosome maintenance (MCM) proteins[33, 34]. The MCM complex has a role in both the initiation and elongation phases of eukaryotic DNA replication[35, 36, 53]. The overlap of genes associated with cell cycle and DNA replication between the Pollard group's microarray results and ours is striking. In the uterine epithelium, E2 stimulates expression of MCMs, while P4 decreases transcripts of MCM2 through MCM6[33, 54]. Our IHC results showed aberrant overexpression of MCM2 and MCM6 in *Mig-6*$^{d/d}$ mice at the pre-implantation stage. A similar action can be ascribed to P4 and E2 in the human endometrial epithelium, since a loss of MCM proteins occurs in the secretory phase, and P4 dominates this phase of the menstrual cycle[7, 37]. However, aberrant overexpression of MCM2 and MCM6 may cause abnormal epithelial proliferation and nonreceptive endometrium in infertile women with endometriosis[38]. Our results regarding MIG-6 and ERBB2/ESR1 signaling in regulating uterine function in response to hormonal signals will bring insight into uterine pathophysiology and likely lead to new therapies for endometrial diseases. Deeper inquiry into endometrial epithelial-stromal crosstalk between ErbB2/ERK/ESR1 and PGR/MIG-6 signaling pathways will be of major importance to understanding infertility and endometriosis.

In summary, our findings reveal that attenuation of MIG-6 occurs both in endometriotic lesions and in the endometriosis-effected eutopic endometrium. Evidence from mice indicates that loss of *Mig-6* in endometriotic lesions promotes their development and accelerates endometriosis-related infertility, while loss of *Mig-6* in the eutopic endometrium causes infertility due to defects in implantation and endometrial receptivity. We found that increased epithelial proliferation caused by *Mig-6* loss is caused by E2 through the ERBB2/ERK pathway (Fig. 6). However, targeting *Erbb2* can reverse all apparent female reproductive defects caused by *Mig-6* loss including endometrial hyperplasia, infertility, and endometriosis lesion development. Attenuation of *Mig-6* causes the inability of P4 to properly control the cell cycle and inhibit E2-induced aberrant epithelial proliferation that results from increases in MCMs. However, counteracting the overexpression of *Erbb2* restores normal gene expression patterns, providing a molecular explanation for the rescue of normal reproductive function. These findings not only elucidate a critical pathway for understanding the hormonal control of normal uterine physiology, but they also provide the potential for new treatment strategies for uterine disease.

Methods

Study design

The main objective of this study was to evaluate the role of MIG-6 in endometrial P4 resistance. First, the expression of MIG-6 was assessed in eutopic endometrium of infertile women with endometriosis compared to fertile women. To determine whether endometriosis affects MIG-6 expression, we examined MIG-6 expression in a nonhuman primate and mouse model of endometriosis. Subsequently, we identified ERBB2 as a MIG-6 target and evaluate the impact of *Erbb2* ablation on the infertility and endometrial P4 resistance of *Mig-6*$^{d/d}$ mice. Finally, transcriptomic analysis was applied to dissect the

molecular mechanisms of *Mig-6* in the uterus. The control and treatment groups and the number of biological replicates (sample sizes) for each experiment are specified in the figure legends. Animal numbers for each study type were determined by the investigators on the basis of previous experience with the standard disease models that were used or from pilot studies. Animals were randomly allocated to the control and treatment groups and housed together to minimize environmental differences and experimental bias. Analysis of endpoint readouts was carried out in a blinded fashion.

Ethics Statement

The institutional review board of Michigan State University, Greenville Health System, and University of North Carolina approved this study. The Institutional Animal Care and Use Committee at Michigan State University approved all experiments relating to mice. The Institutional Animal Care and Use Committees of both the University of Illinois at Chicago and Michigan State University approved the endometriosis baboon animal model.

Human Endometrium Samples

The human endometrial samples used to examine MIG-6 expression patterns were obtained from Michigan State University's Center for Women's Health Research Female Reproductive Tract Biorepository, the University of North Carolina, and the Greenville Hospital System in accordance with the guidelines set by the Institutional Review Boards of Michigan State University (Grand Rapids, MI), the University of North Carolina (Chapel Hill, NC), and Greenville Health System (Greenville, SC), respectively. Written informed consent was obtained from all participants. For experiments examining *MIG-6* mRNA expression throughout the menstrual cycle, endometrial samples were analyzed from 22 cycling premenopausal women without endometriosis (n = 6 proliferative, n = 7 early secretory, n = 3 mid secretory, and n = 6 late secretory) and from 20 cycling premenopausal women with endometriosis (n = 2 proliferative, n = 6 early secretory, n = 9 mid secretory, and n = 3 late secretory). Control endometrial tissues were laparoscopically negative for endometriosis and had not been on any hormonal therapies for at least three months prior to surgery. Endometrial menstrual staging was confirmed by an experienced pathologist familiar with female reproduction. To investigate MIG-6 amounts in the endometrium from women, 10 control and 10 eutopic endometrium with endometriosis were used. To compare MIG-6 amounts in the eutopic endometrium and ectopic lesions of women with endometriosis, each of 12 samples were used. All women with endometriosis were infertile. Samples used for immunohistochemistry were fixed in 10% buffered formalin prior to embedding in paraffin wax.

Animals And Tissue Collection

Animals were maintained in a designated animal care facility according to Michigan State University's Institutional Guidelines for the care and use of laboratory animals. All animal procedures were approved by the Institutional Animal Care and Use Committee of Michigan State University. For all animal studies, animals were randomly distributed among different conditions by the investigator as the animals did not show any size or appearance differences at the onset of the experiments. No animals were excluded, and the investigator was not blinded to group allocation during the experiment. *Erbb2* conditional knockout

mice were generated by crossing *Pgr*$^{cre/+}$*Mig-6*$^{f/f}$ with *Erbb2*$^{f/f}$ mice (*Pgr*$^{cre/+}$*Mig-6*$^{f/f}$*Erbb2*$^{f/f}$; *Mig-6*$^{d/d}$*Erbb2*$^{d/d}$). Pregnant uterine samples were obtained by mating control (*Mig-6*$^{f/f}$ or *Mig-6*$^{f/f}$*Erbb2*$^{f/f}$), *Mig-6*$^{d/d}$ and *Mig-6*$^{d/d}$*Erbb2*$^{d/d}$ female mice with C57BL/6 male mice the morning of a vaginal plug designated as day 0.5 of gestation (GD 0.5). Mice were sacrificed at GD 3.5 and 5.5. For the study of steroid hormone regulation, control, *Mig-6*$^{d/d}$ and *Mig-6*$^{d/d}$*Erbb2*$^{d/d}$ mice at 6 weeks of age were ovariectomized. Two weeks postsurgery, ovariectomized mice were injected with vehicle (sesame oil; Veh) or estradiol (0.1 μg/mouse; E2) plus progesterone (1 mg/mouse; P4) for 3 days and euthanized at 6 hours after injection. For the fertility studies, adult female control, *Mig-6*$^{d/d}$ and *Mig-6*$^{d/d}$*Erbb2*$^{d/d}$ mice were placed with wild type C57BL/6 male mice. The mating cages were maintained for 6 months and the number of litters and pups born during that period was recorded. Uterine tissues were then immediately processed at the time of dissection and either fixed with 4% (vol/vol) paraformaldehyde for histology or immunohistochemistry or snap frozen and stored at -80 °C for RNA/protein extraction.

Induction Of Endometriosis

For baboon uterine samples, endometriosis was induced by intraperitoneal inoculation of menstrual endometrium on two consecutive menstrual cycles and harvested using laparotomy via endometriectomy from four female baboons as previously described [55]. For mouse uterine samples, 8-weeks-old female mice which have conditional double-fluorescent Cre reporter gene (*Pgr*$^{cre/+}$*Rosa26*^{mTmG}, *Pgr*$^{cre/+}$ *Mig-6*$^{f/f}$*Rosa26*^{mTmG}, and *Pgr*$^{cre/+}$ *Mig-6*$^{f/f}$*Erbb2*$^{f/f}$ *Rosa26*^{mTmG} were injected with 1 μg/ml of E2 per a day at three times and had a surgical procedure to induce endometriosis. Under anesthesia, a midline abdominal incision was made to expose the uterus in female mice, and one of uterine horn was removed. In a Petri dish containing phosphate-buffered saline (PBS; pH 7.5), the uterine horn was opened longitudinally with scissors. The excised uterine horn was cut into small fragments of about 1 mm^3, and then injected back into the peritoneum of same mouse. The abdominal incision and wound were closed with sutures and skin was closed with surgical wound clips, respectively. After a designated time, the mice were euthanized, and endometriosis-like lesions were removed using a fluorescence microscope and counted.

Endometriosis-related Infertility Analysis

Endometriosis were induced in 8 week old control female mouse recipient (fertile) receiving endometrial fragments from donor control (*Pgr*$^{cre/+}$*Rosa26*^{mTmG}) or *Mig-6*$^{d/d}$ *Rosa26*^{mTmG} endometrium. A sham surgery group was included as a control. After 1, 2, and 3 months of the endometriosis induction, the mice with endometriotic lesions of control or *Mig-6*$^{d/d}$ were mated with wild-type male mice and then collected at GD 7.5.

RNA Isolation And Microarray Analysis

Total RNA was extracted from the uterine tissues using the RNeasy Total RNA Isolation Kit (Qiagen, Valencia, CA). RNA was pooled from the uteri of more than three mice per genotype at GD 3.5 and microarray analysis was performed using GeneChip® Mouse Genome 430 2.0 Arrays (Affymetrix) as

described previously [56](Gene Expression Omnibus accession code GSE138185). Array data were analyzed using Bioconductor for quantile normalization. We selected aberrantly expressed genes in the uteri of control, *Mig-6*$^{d/d}$ and *Mig-6*$^{d/d}$*Erbb2*$^{d/d}$ mice at GD 3.5 using a two-sample comparison according to significant fold change greater than 1.5. Aberrantly expressed genes were classified with canonical pathway analyzed by Ingenuity System Software (Ingenuity Systems Inc.).

Reverse Transcription - Quantitative PCR

The complementary DNAs (cDNAs) were synthesized with MMLV Reverse Transcriptase (Invitrogen Crop) according to the manufacturer's instructions. RT-qPCR was performed on cDNA to assess the expression of genes of interest with SYBR Green (Bio-Rad) or TaqMan primers (Applied Biosystems). Experimental gene expression data were normalized against the housekeeping gene, 18S ribosomal RNA. Analysis of mRNA expression was first undertaken by the standard curve method, and results were corroborated by cycle threshold values assessing gene expression. Primer sequences used in these studies are shown in table S4.

Immunohistochemistry Analyses

Immunohistochemistry and immunofluorescence analyses were performed as previously described [57]. Briefly, dewaxed hydrated paraffin-embedded tissue sections were pre-incubated with 10% normal goat (for anti-MIG-6, Ki67, Cyclin D1, ErbB2, pERK1/2, ERK1/2, MUC1, LTF, and KLF4 antibodies) or donkey (for anti-MCM2, MCM6, and KLF15 antibodies) serum in PBS and then incubated with anti-MIG-6 (1:200 dilution; Customized antibody by Dr. Jeong Lab), anti-Ki67 (1:1000 dilution; #ab15580; Abcam), anti-Cyclin D1 (1:1000 dilution; #eo-RB9041-p0; Thermo Fisher Scientific), anti-ErbB2 (1:200 dilution; #2165; Cell Signaling), anti-pERK1/2 (1:500 dilution; #4370; Cell Signaling), anti-ERK1/2 (1:1000 dilution; #4695; Cell Signaling), anti-MUC1 (1:1000 dilution; #ab15481, Abcam), anti-LTF (1:2000 dilution; #07-682, Millipore Corp.), anti-MCM2 (1:20000 dilution; #sc9839, Santa Cruz Biotechnology), anti-MCM6 (1:20000 dilution; #sc9843; Santa Cruz Biotechnology), anti-KLF4 (1:5000 dilution; #sc20691; Santa Cruz Biotechnology), and anti-KLF15 (1:5000 dilution; #ab2647; Abcam) antibodies in PBS supplemented with 10% normal serum overnight at 4 °C. For immunohistochemistry, the sections were incubated with secondary antibody conjugated to horseradish peroxidase (Vector Laboratories) for one hour at room temperature. Immunoreactivity was detected using diaminobenzidine (DAB-Vector Laboratories) and analyzed using microscopy software from NIS Elements, Inc. (Nikon). A semi-quantitative grading system (H-score) was calculated to compare the immunohistochemical staining intensities. The H-score was calculated using the following equation: H-score = $\sum$ Pi (i), where i = intensity of staining with a value of 1, 2, or 3 (weak, moderate, or strong, respectively) and Pi is the percentage of stained cells for each intensity, varying from 0 to 100%. The overall score ranged from 0 to 300 [58].

Western Blot Analysis

Western blot analyses were performed as described previously [59]. Proteins were extracted using lysis buffer (10 mM Tris-HCl (pH 7.4), 150 mM NaCl, 2.5 mM EDTA, and 0.125% Nonidet P-40 (vol/vol)) supplemented with both a protease inhibitor cocktail (Roche, Indianapolis, IN) and a phosphatase inhibitor cocktail (Sigma-Aldrich, St. Louis, MO). Protein lysates were electrophoresed via SDS-PAGE and transferred onto polyvinylidene difluoride membrane (Millipore Corp., Bedford, MA). Membrane was blocked with Casein (0.5% w/v) in PBS with 0.1% Tween 20 (v/v; Sigma-Aldrich) prior to exposure to anti-ErbB2 (#2165; Cell Signaling, Danvers, MA), anti-EGFR (#2646; Cell Signaling), anti-phospho-ERK1/2 (pERK1/2; #4370; Cell Signaling), anti-ERK1/2 (#4695; Cell Signaling), anti-MIG-6 (Customized antibody by Dr Jeong Lab) or anti-β-actin (#sc1616; Santa Cruz Biotechnology) antibodies diluted to 1:1000. Immunoreactivity was visualized by incubation with a horseradish peroxidase-linked secondary antibody followed by exposure to Electrochemiluminescence reagents (ECL) according to manufacturer's instructions (GE Healthcare Biosciences).

Statistical Analysis

No statistical method was used to predetermine sample size for in vivo studies. Based on prior experience, all experiments used 5 mice per group to achieve adequate statistical power. For all animal experiments, block randomization was used to ensure a balance in sample size across groups. The investigators were blinded during the evaluation of results variations in the group. For all animal experiments, over three biological replicates were analyzed for each condition, and results are presented as the mean ± SEM. For data with only two groups, Student's t test was used. For data containing more than two groups, an analysis of variance (ANOVA) test was used, followed by Tukey test for pairwise t-test. $p < 0.05$ was considered statistically significant. All statistical analyses were performed using the Instat package from GraphPad. The original data are provided in table S5.

Data Availability

All data are available in the manuscript or the supplementary material. The accession number for microarray generated in this study is GSE138185.

Declarations

Competing interests:

The authors declare that they have no competing interests.

Funding:

This work was supported by the National Research Foundation of Korea (NRF) grant funded by the Korean Government (MIST) (No. 2018R1A5A2025079 to H.G.Y.), and SRI and Bayer Discovery/Innovation Grant (to T.H.K.), as well as by the Eunice Kennedy Shriver National Institute of Child Health & Human Development of the National Institutes of Health under Award Number R01HD084478 and R01HD101243 (to J.W.J) and F31HD101207 and T32HD087166 (to R.M.M.). The content is solely the responsibility of the authors and does not necessarily represent the official views of the National Institutes of Health.

Author contributions:

H.-G.Y. and J.-W.J. were responsible for the concept of the study; A.T.F. collected baboon samples; S.L.Y. and B.A.L. collected human samples; J.-Y.Y. and T.H.K. carried out experiments; J.-Y.Y., T.H.K. and J.-H.S. analyzed data; U.M. provided transgenic mice; R.M.M. contributed to write the manuscript. All authors contributed to the final manuscript version.

Ethics declarations

Competing interests: The authors declare that they have no competing interests.

References

1. McKinnon B, Mueller M, Montgomery G. Progesterone Resistance in Endometriosis: an Acquired Property? *Trends in endocrinology and metabolism: TEM* **29**, 535-548 (2018).
2. Al-Sabbagh M, Lam EW, Brosens JJ. Mechanisms of endometrial progesterone resistance. *Molecular and cellular endocrinology* **358**, 208-215 (2012).
3. Aghajanova L, Velarde MC, Giudice LC. Altered gene expression profiling in endometrium: evidence for progesterone resistance. *Semin Reprod Med* **28**, 51-58 (2010).
4. Pijnenborg JM*, et al.* Aberrations in the progesterone receptor gene and the risk of recurrent endometrial carcinoma. *J Pathol* **205**, 597-605 (2005).
5. Lessey BA, Kim JJ. Endometrial receptivity in the eutopic endometrium of women with endometriosis: it is affected, and let me show you why. *Fertility and sterility* **108**, 19-27 (2017).
6. Patel BG, Rudnicki M, Yu J, Shu Y, Taylor RN. Progesterone resistance in endometriosis: origins, consequences and interventions. *Acta Obstet Gynecol Scand* **96**, 623-632 (2017).
7. Lessey BA, Young SL. Homeostasis imbalance in the endometrium of women with implantation defects: the role of estrogen and progesterone. *Semin Reprod Med* **32**, 365-375 (2014).
8. Marquardt RM, Kim TH, Shin JH, Jeong JW. Progesterone and Estrogen Signaling in the Endometrium: What Goes Wrong in Endometriosis? *International journal of molecular sciences* **20**, (2019).
9. Li X, Feng Y, Lin JF, Billig H, Shao R. Endometrial progesterone resistance and PCOS. *J Biomed Sci* **21**, 2 (2014).
10. Fox C, Morin S, Jeong JW, Scott RT, Jr., Lessey BA. Local and systemic factors and implantation: what is the evidence? *Fertility and sterility* **105**, 873-884 (2016).
11. Burney RO*, et al.* Gene expression analysis of endometrium reveals progesterone resistance and candidate susceptibility genes in women with endometriosis. *Endocrinology* **148**, 3814-3826 (2007).
12. Kao LC*, et al.* Expression profiling of endometrium from women with endometriosis reveals candidate genes for disease-based implantation failure and infertility. *Endocrinology* **144**, 2870-2881 (2003).

13. Eskenazi B, Warner ML. Epidemiology of endometriosis. *Obstetrics and gynecology clinics of North America* **24**, 235-258 (1997).
14. Bulun SE. Endometriosis. *The New England journal of medicine* **360**, 268-279 (2009).
15. Kaunitz AM. Injectable depot medroxyprogesterone acetate contraception: an update for U.S. clinicians. *Int J Fertil Womens Med* **43**, 73-83 (1998).
16. Olive DL, Lindheim SR, Pritts EA. New medical treatments for endometriosis. *Best Pract Res Clin Obstet Gynaecol* **18**, 319-328 (2004).
17. Bulun SE*, et al.* Progesterone resistance in endometriosis: link to failure to metabolize estradiol. *Molecular and cellular endocrinology* **248**, 94-103 (2006).
18. Berkley KJ, Rapkin AJ, Papka RE. The pains of endometriosis. *Science* **308**, 1587-1589 (2005).
19. Jeong JW*, et al.* Identification of murine uterine genes regulated in a ligand-dependent manner by the progesterone receptor. *Endocrinology* **146**, 3490-3505 (2005).
20. Jeong JW*, et al.* Mig-6 modulates uterine steroid hormone responsiveness and exhibits altered expression in endometrial disease. *Proc Natl Acad Sci U S A* **106**, 8677-8682 (2009).
21. Braundmeier AG, Fazleabas AT. The non-human primate model of endometriosis: research and implications for fecundity. *Molecular human reproduction* **15**, 577-586 (2009).
22. Fazleabas AT, Brudney A, Gurates B, Chai D, Bulun S. A modified baboon model for endometriosis. *Annals of the New York Academy of Sciences* **955**, 308-317; discussion 340-302, 396-406 (2002).
23. Finn CA, Martin L. Endocrine control of the timing of endometrial sensitivity to a decidual stimulus. *Biology of reproduction* **7**, 82-86 (1972).
24. Tan J, Paria BC, Dey SK, Das SK. Differential uterine expression of estrogen and progesterone receptors correlates with uterine preparation for implantation and decidualization in the mouse. *Endocrinology* **140**, 5310-5321 (1999).
25. Brenner RM, West NB, McClellan MC. Estrogen and progestin receptors in the reproductive tract of male and female primates. *Biology of reproduction* **42**, 11-19 (1990).
26. Lee CH*, et al.* Extracellular signal-regulated kinase 1/2 signaling pathway is required for endometrial decidualization in mice and human. *PLoS One* **8**, e75282 (2013).
27. Lessey BA, Young SL. What exactly is endometrial receptivity? *Fertility and sterility* **111**, 611-617 (2019).
28. Vasquez YM, DeMayo FJ. Role of nuclear receptors in blastocyst implantation. *Seminars in cell & developmental biology* **24**, 724-735 (2013).
29. Bhurke AS, Bagchi IC, Bagchi MK. Progesterone-Regulated Endometrial Factors Controlling Implantation. *American journal of reproductive immunology* **75**, 237-245 (2016).
30. Hantak AM, Bagchi IC, Bagchi MK. Role of uterine stromal-epithelial crosstalk in embryo implantation. *The International journal of developmental biology* **58**, 139-146 (2014).
31. Cha J, Sun X, Dey SK. Mechanisms of implantation: strategies for successful pregnancy. *Nature medicine* **18**, 1754-1767 (2012).

32. Kim TH, Lee DK, Franco HL, Lydon JP, Jeong JW. ERBB receptor feedback inhibitor 1 regulation of estrogen receptor activity is critical for uterine implantation in mice. *Biology of reproduction* **82**, 706-713 (2010).
33. Pan H, Deng Y, Pollard JW. Progesterone blocks estrogen-induced DNA synthesis through the inhibition of replication licensing. *Proc Natl Acad Sci U S A* **103**, 14021-14026 (2006).
34. Tong W, Pollard JW. Progesterone inhibits estrogen-induced cyclin D1 and cdk4 nuclear translocation, cyclin E- and cyclin A-cdk2 kinase activation, and cell proliferation in uterine epithelial cells in mice. *Mol Cell Biol* **19**, 2251-2264 (1999).
35. Hyrien O. How MCM loading and spreading specify eukaryotic DNA replication initiation sites. *F1000Res* **5**, (2016).
36. Das SP, Rhind N. How and why multiple MCMs are loaded at origins of DNA replication. *Bioessays* **38**, 613-617 (2016).
37. Niklaus AL*, et al.* Assessment of the proliferative status of epithelial cell types in the endometrium of young and menopausal transition women. *Human reproduction* **22**, 1778-1788 (2007).
38. Ray S, Pollard JW. KLF15 negatively regulates estrogen-induced epithelial cell proliferation by inhibition of DNA replication licensing. *Proc Natl Acad Sci U S A* **109**, E1334-1343 (2012).
39. Kurita T, Lee KJ, Cooke PS, Lydon JP, Cunha GR. Paracrine regulation of epithelial progesterone receptor and lactoferrin by progesterone in the mouse uterus. *Biol Reprod* **62**, 831-838 (2000).
40. Bigsby RM, Caperell-Grant A, Berry N, Nephew K, Lubahn D. Estrogen induces a systemic growth factor through an estrogen receptor-alpha-dependent mechanism. *Biol Reprod* **70**, 178-183 (2004).
41. Fazleabas AT. A baboon model for simulating pregnancy. *Methods in molecular medicine* **121**, 101-110 (2006).
42. Fazleabas AT. A baboon model for inducing endometriosis. *Methods in molecular medicine* **121**, 95-99 (2006).
43. D'Hooghe TM, Bambra CS, Suleman MA, Dunselman GA, Evers HL, Koninckx PR. Development of a model of retrograde menstruation in baboons (Papio anubis). *Fertility and sterility* **62**, 635-638 (1994).
44. Grummer R. Animal models in endometriosis research. *Human reproduction update* **12**, 641-649 (2006).
45. Giudice LC, Kao LC. Endometriosis. *Lancet* **364**, 1789-1799 (2004).
46. Bruner-Tran KL, Mokshagundam S, Herington JL, Ding T, Osteen KG. Rodent Models of Experimental Endometriosis: Identifying Mechanisms of Disease and Therapeutic Targets. *Curr Womens Health Rev* **14**, 173-188 (2018).
47. Lin YJ, Lai MD, Lei HY, Wing LY. Neutrophils and macrophages promote angiogenesis in the early stage of endometriosis in a mouse model. *Endocrinology* **147**, 1278-1286 (2006).
48. Fang Z*, et al.* Intact progesterone receptors are essential to counteract the proliferative effect of estradiol in a genetically engineered mouse model of endometriosis. *Fertility and sterility* **82**, 673-678

(2004).
49. Fang Z*, et al.* Genetic or enzymatic disruption of aromatase inhibits the growth of ectopic uterine tissue. *The Journal of clinical endocrinology and metabolism* **87**, 3460-3466 (2002).
50. Foster WG, Ruka MP, Gareau P, Foster RA, Janzen EG, Yang JZ. Morphologic characteristics of endometriosis in the mouse model: application to toxicology. *Can J Physiol Pharmacol* **75**, 1188-1196 (1997).
51. Cummings AM, Metcalf JL, Birnbaum L. Promotion of endometriosis by 2,3,7,8-tetrachlorodibenzo-p-dioxin in rats and mice: time-dose dependence and species comparison. *Toxicol Appl Pharmacol* **138**, 131-139 (1996).
52. Wu SP, Li R, DeMayo FJ. Progesterone Receptor Regulation of Uterine Adaptation for Pregnancy. *Trends in endocrinology and metabolism: TEM* **29**, 481-491 (2018).
53. Slaymaker IM, Chen XS. MCM structure and mechanics: what we have learned from archaeal MCM. *Subcell Biochem* **62**, 89-111 (2012).
54. Pan H, Zhu L, Deng Y, Pollard JW. Microarray analysis of uterine epithelial gene expression during the implantation window in the mouse. *Endocrinology* **147**, 4904-4916 (2006).
55. Afshar Y, Hastings J, Roqueiro D, Jeong JW, Giudice LC, Fazleabas AT. Changes in eutopic endometrial gene expression during the progression of experimental endometriosis in the baboon, Papio anubis. *Biology of reproduction* **88**, 44 (2013).
56. Yoo JY, Kim TH, Lee JH, Dunwoodie SL, Ku BJ, Jeong JW. Mig-6 regulates endometrial genes involved in cell cycle and progesterone signaling. *Biochemical and biophysical research communications* **462**, 409-414 (2015).
57. Kim BG*, et al.* Aberrant activation of signal transducer and activator of transcription-3 (STAT3) signaling in endometriosis. *Human reproduction* **30**, 1069-1078 (2015).
58. Ishibashi H*, et al.* Sex steroid hormone receptors in human thymoma. *The Journal of clinical endocrinology and metabolism* **88**, 2309-2317 (2003).
59. Kim TH*, et al.* ARID1A Is Essential for Endometrial Function during Early Pregnancy. *PLoS genetics* **11**, e1005537 (2015).

Figures

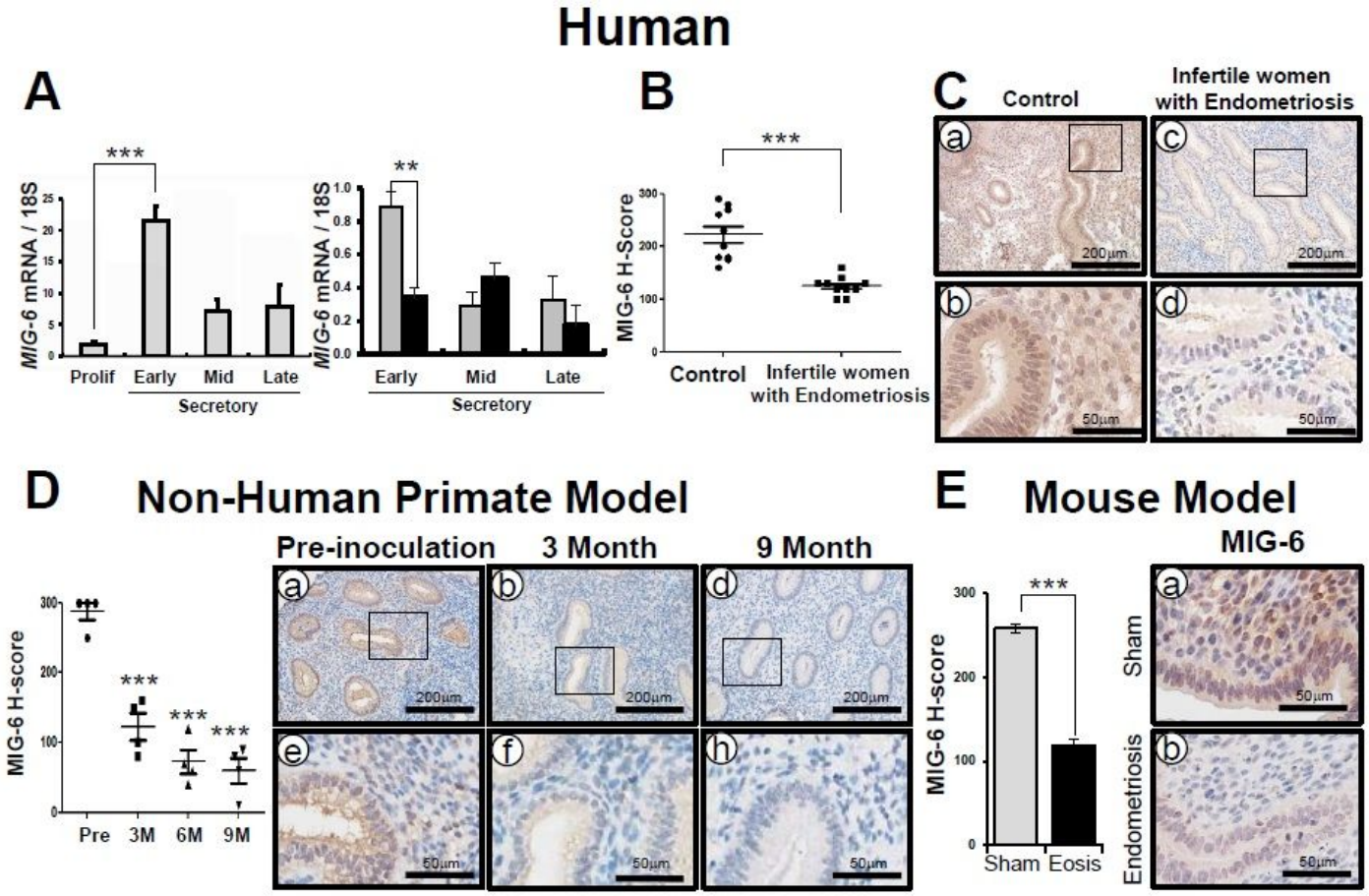

Figure 1

MIG-6 expression in the endometrium of women with endometriosis and nonhuman primate, baboon model. (A), RT-qPCR analysis of MIG-6 gene expression in endometrium from women with and without endometriosis during the menstrual cycle (n ≥ 3 for each group). (B), (C), Immunohistochemical H-score (B) and representative photomicrographs (C) of MIG-6 in the endometrium from women with endometriosis as compared to control (n = 10 for each group). (D), Immunohistochemical H-score and representative photomicrographs of MIG-6 in the endometriosis baboon model induced by intraperitoneal inoculation of menstrual endometrium during progression of endometriosis in pre-inoculation, 3, 6, and 9 months (n = 4 per period). €, Immunohistochemical H-score and representative photomicrographs of MIG-6 in the endometriosis mouse model (n = 5 for group). Mean ± SEM, ** P<0.01 and *** P<0.001, Student's t test for data containing only two groups and ANOVA followed by Tukey test for pairwise t-test for data containing more than two groups.

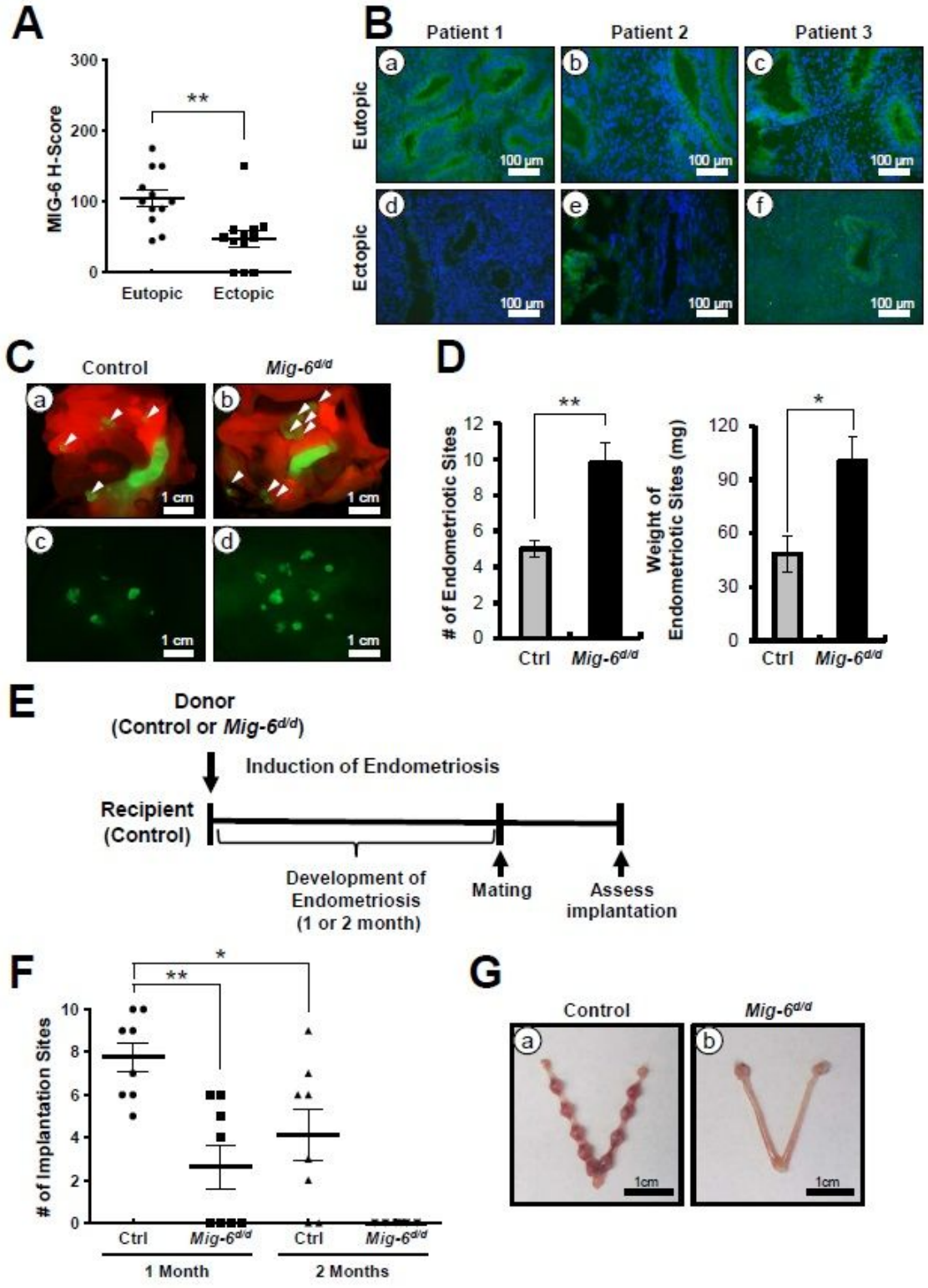

Figure 2

Reduction of MIG-6 in ectopic lesions in endometriosis patients and the effect of ectopic lesions with MIG-6 deficiency on endometriosis development and embryo implantation. (A), (B), Decrease of MIG-6 expression in ectopic endometriotic lesions compared to eutopic endometrium from the same endometriosis patients. H-score (A) and representative photomicrographs (B) of immunofluorescence analysis of MIG-6 in eutopic endometrium and ectopic lesions from women with endometriosis (n=10).

(C), (D), The effect of ectopic lesions with MIG-6 deficiency on endometriosis development. Endometriosis was surgically induced in control (Pgrcre/+Rosa26mTmG/+) and Mig-6d/dRosa26mTmG/+ mice. Fluorescence photomicrographs (C) and average total number (D) of endometriosis lesions in control and Mig-6d/dRosa26mTmG/+ mice (n=5). (E), (F), (G), The effect of ectopic lesions with MIG-6 deficiency on embryo implantation. (E) Experimental design to access the effect of ectopic lesions with MIG-6 deficiency on embryo implantation. Average number (F) and uterine images (G) of implantation sites at GD 7.5 in mice with endometriosis on 1 and 3 months after endometriosis induction (n=5 or more per period). Mean ± SEM, ** $p<0.01$ and *** $p<0.001$, Student's t test for data containing only two groups and ANOVA followed by Tukey test for data containing more than two groups.

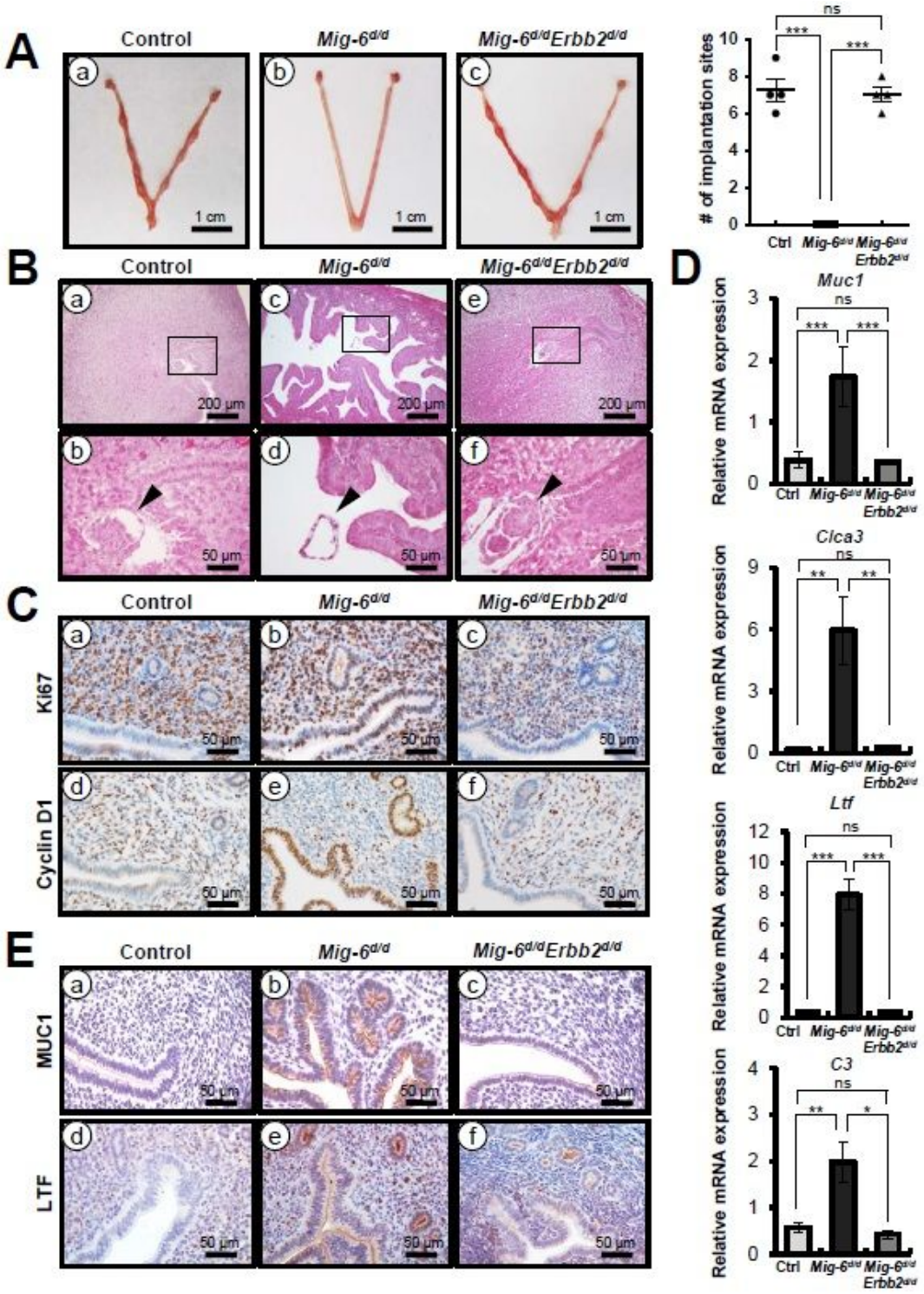

Figure 3

Rescue of implantation defect and recovery of aberrant activated epithelial cells proliferation and ESR signaling in Mig-6d/d mice by Erbb2 double ablation. (A), Uteri of control, Mig-6d/d, and Mig-6d/dErbb2d/d mice and number of implantation sites at GD 5.5 (n=4 for each genotype). (B), Hematoxylin and eosin (H&E) staining in paired endometrium of control, Mig-6d/d, and Mig-6d/dErbb2d/d mice at GD 5.5. Arrowheads indicate embryos. (C), Immunohistochemistry analysis of Ki67

and Cyclin D1 in the endometrium of control, Mig-6d/d, and Mig-6d/dErbb2d/d mice at GD 3.5. (D), (E), RT-qPCR analysis of Muc1, Clca3, Ltf, and C3 (D) and immunohistochemistry analysis of MUC1 and LTF (E) as epithelial ESR1 target genes in the uterus of control, Mig-6d/d, and Mig-6d/dErbb2d/d mice at GD 3.5 (n = 6 for each genotype). Mean ± SEM, * P<0.05, ** P<0.01, and *** P<0.001, ANOVA followed by Tukey test.

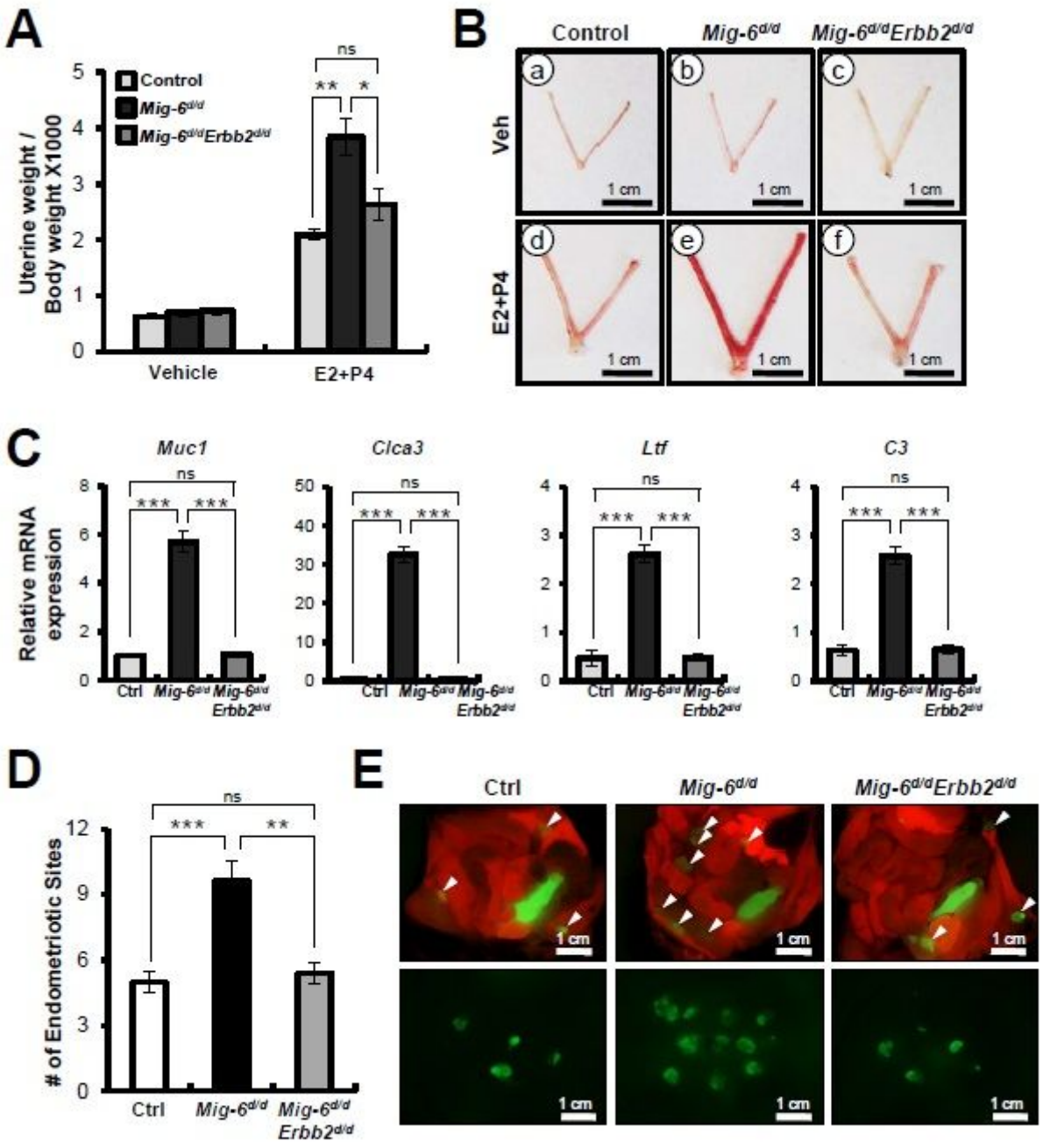

Figure 4

Rescue of steroid hormone dysregulation in Mig-6d/d mice by Erbb2 double ablation. (A), (B), Ratio of uterine weight to body weight (A) and uteri (B) of control, Mig-6d/d, and Mig-6d/dErbb2d/d mice treated

with vehicle or E2+P4 for 3 days (n = 3 or more for each group). (C), RT-qPCR analysis of epithelial ESR1 target genes expression, Muc1, Clca3, Ltf, and C3 in the uteri of control, Mig-6d/d, and Mig-6d/dErbb2d/d mice treated with E2+P4 for 3 days (n = 5 per genotype). (D), €, Average total number (D) and representative fluorescence photomicrographs (E) of endometriotic sites in control, Mig-6d/d, and Mig-6d/dErbb2d/d mice by induced endometriosis based on mT/mG mice (n = 5 per genotype). Arrowheads indicate lesions attached to the outside of uterus. Mean ± SEM, * P<0.05, ** P<0.01, and *** P<0.001, ANOVA followed by Tukey test.

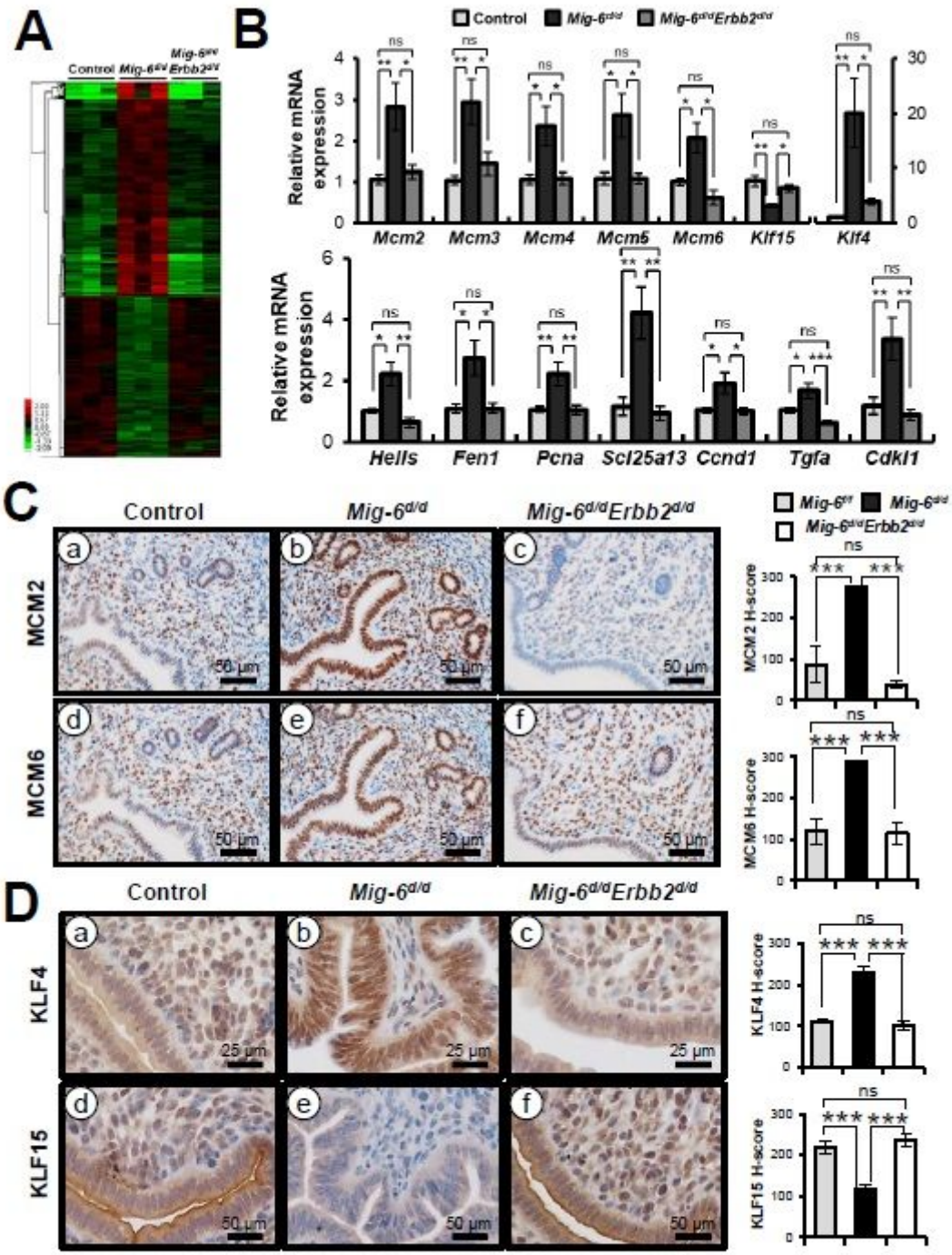

Figure 5

Recovery of gene expression (Microarray) in Mig-6d/d mice by Erbb2 double ablation. (A), Clustering analysis of Mig-6 dependent regulated genes in uteri of control, Mig-6d/d, and Mig-6d/dErbb2d/d mice at GD 3.5. The extent of gene expression changes is represented by a green-red color scale (green: low expression and red: high expression). (B), RT-qPCR analysis of transcript amounts of Mig-6 dependent regulated genes in uteri of control, Mig-6d/d, and Mig-6d/dErbb2d/d mice at GD 3.5 (n = 5 or 6 per each genotype). Mean ± SEM, * P<0.05, ** P<0.01, and *** P<0.001, ANOVA followed by Tukey test. (C), Immunohistochemistry analysis of MCM2 and MCM6 in the uterus of control, Mig-6d/d, and Mig-6d/dErbb2d/d mice at GD 3.5. (D), Immunohistochemistry analysis of KLF4 and KLF15 in the uterus of control, Mig-6d/d, and Mig-6d/dErbb2d/d mice at GD 3.5.

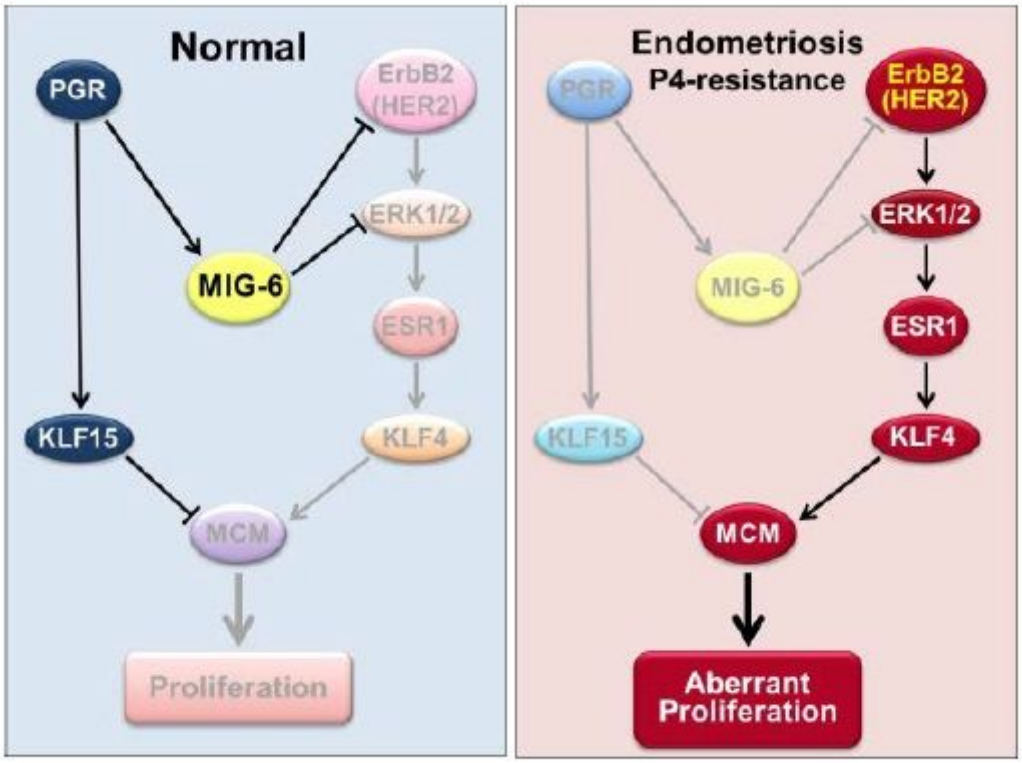

Figure 6

Molecular mechanisms of MIG-6 function in the uterus. MIG-6 mediates P4 inhibition of E2 signaling by inhibiting ErbB2-ERK signaling (Left side), and the attenuation of MIG-6 leads to ErbB2-ERK activation, proliferation of uterine epithelial cells, and eventually to endometriosis and infertility (Right side).

Supplementary Files

This is a list of supplementary files associated with this preprint. Click to download.

- Mig6ErbB2FigureNatureCommunicationSupplementarydata.docx